UDC 629.3.027.4:625.731.2
DOI: 10.15587/2706-5448.2025.329471

Volodymyr Kovbasa,
Nataliia Priliepo

DETERMINATION OF ANALYTICAL DEPENDENCIES OF DISTRIBUTED FORCES IN A DEFORMABLE WHEEL – DEFORMABLE SURFACE CONTACT ZONE

The object of this study is the contact interaction of two deformable bodies of inconsistent geometric shape, in particular, change in the stress-strain state of the wheel and the supporting surface. The significance of this topic arises from growing demands for vehicle mobility in difficult terrains, the necessity of minimizing environmental impact, and the need to optimize the design of mobile machinery components. A major challenge lies in developing a suitable analytical solution to define the stress-strain state variations within the contact zone between the wheel and soil or other surfaces.

This study employs an approach grounded in the fundamental principles of mathematical physics applied to elasticity theory problems. This enabled the derivation of analytical equations that describe the absolute deformations of both the surface and the wheel (tire), along with the contact pressure distribution. The pressure distribution within the contact zone was determined using the properties of surface integrals of the second kind. Concentrated forces, when related to the contact area, were equated to the integral value of this surface integral. The values of these distributed forces were then incorporated into the transformed Boussinesq and Cerruti potential equations.

The resulting analytical relationships can be utilized to determine the relative deformations of the contacting bodies and the stress distribution within them. Crucially, these relationships also serve as a basis for deriving equations that define the contact zone boundaries and the rolling resistance coefficient for deformable bodies. These derived relationships are general and presented in a form applicable to loads on both driving and passive (driven) wheels.

This proposed model offers substantially improved analytical accuracy over existing empirical methods. Moreover, these analytical dependencies help circumvent the computationally intensive calculations typically required by FEM (Finite Element Method) or DEM (Discrete Element Method) simulations for every unique loading scenario and material property set.

Keywords: *deformable wheel, deformable surface, soil compaction, contact surface, contact zone.*

Received: 01.03.2025
Received in revised form: 18.04.2025
Accepted: 09.05.2025
Published: 19.05.2025

How to cite
Kovbasa, V., Priliepo, N. (2025). Determination of analytical dependencies of distributed forces in a deformable wheel – deformable surface contact zone. Technology Audit and Production Reserves, 3 (1 (83)), 6–12. https://doi.org/10.15587/2706-5448.2025.329471

1. Introduction

When solving problems related to the machines and wheels' interaction with soil, methods of continuum mechanics can be used under the assumption that the soil is formalized as a quasi-continuous deformable medium. In this case, applying physical equations for stresses and deformations or deformation rates is necessary. Such relationships can manifest themselves in elastic, viscous, or plastic manifestations. Formalizing these manifestations is described by the equations of elasticity, viscosity, plasticity, or their joint expression. Such equations, especially considering several indications of the solid properties, are essentially nonlinear, and their solution is associated with difficulties.

Accordingly, it is essential to identify the fundamental properties and proceed to simplified equations describing the relationship between stresses and deformations (or strain rates). In any case, the basic equations defining the relationship between stress and strain (or strain rate) must be included in the basic equations of dynamics (or statics) for a continuous medium. This inherently allows for the emergence of significant nonlinearities in specific soil properties, often expressed in the form of third-order hyperbolic partial differential equations.

Thus, a thorough investigation of the constitutive equations describing the stress-strain (or strain rate) relationship is required to capture the most influential effects of soil behavior. In this framework, the soil is modelled as a quasi-continuous medium exhibiting elastic, viscous, and plastic characteristics. This approach was previously implemented in different researchers' works [1, 2].

This study focuses on the analytical investigation of the contact interaction between a deformable wheel (tire) and a deformable surface within the bounds of the elasticity theory. The study aims to determine their absolute deformations, serving as essential prerequisites for defining the contact zone boundaries and the rolling resistance coefficient.

Some researchers solve similar problems by representing the tire as an absolutely rigid body, which significantly simplifies the solution, but in this case, the results of experimental studies are significantly different [3].

While analytical methods are available for solving contact problems within the elastic regime, they often neglect pertinent acting forces and incorporate simplifications that can substantially diminish their predictive accuracy [4, 5]. Known methods for solving such problems are deeply analyzed in the publication [6].

Consequently, recent research has increasingly favored numerical solutions, particularly those employing the Finite Element Method (FEM)

and the Discrete Element Method (DEM), over these traditional analytical techniques for modeling such interactions. Nevertheless, a primary limitation of these numerical approaches is their inability to yield general analytical solutions, as they typically provide results specific to the parameters and geometry of the modeled scenario [7, 8].

Considering the increasing requirements for the trafficability of machinery under actual operating conditions, the need to reduce the negative environmental impact, and the need for optimization of the designs of machine propulsion elements, solving the problem of investigating the changes in the stress-strain state of the supporting surface (soil) and the wheel (tire) in their contact zone is highly relevant.

Contact problems involving deformable bodies with deformable surfaces of non-conformal geometric shapes in the contact zone are among the most complex issues in contact mechanics interaction. Furthermore, only analytical methods for solving such problems allow for the determination of rational geometric dimensions and parameters of the deformable wheel for specific loads and mechanical properties of the supporting surface [9, 10].

Thus, *the aim of research* is to reduce the detrimental effect of wheeled propulsion systems on the supporting surface and to increase the energy efficiency of these propulsion systems by developing analytical methods for determining the parameters of contact mechanics interaction between a deformable wheel and a deformable surface, as well as the changes in the stress-strain state of the contacting bodies.

2. Materials and Methods

A significant drawback of this approach is the lack of solution generality since the final solution describes the result corresponding to one specific set of parameters and modes of interaction of the wheel (tire) with a specific mechanical properties surface.

Previous publications showed that, as a first approximation, the interaction of an elastic wheel with an elastic half-space (soil) could be solved as a linear elastic problem with physical linearity and geometric nonlinearity [11].

During the research, analytical methods of mathematical physics were employed, specifically, the classical methods of the theory of elasticity, theoretical and analytical mechanics, mathematical analysis, and mathematical physics.

Analytical dependencies were derived to determine the effect of concentrated forces applied to the wheel axle and the torque acting on it on the distribution of forces within the contact zone of deformable bodies with non-conformal geometric shapes, particularly the deformable wheel (tire) and the deformable supporting surface.

These dependencies enabled the derivation of analytical relationships for determining the absolute deformations of the deformable wheel and the deformable surface in the contact zone. The analytical dependencies account for the weight loads on the wheel, torque, traction resistance referred to the wheel axle, pushing force (for a passive wheel), the geometric dimensions of the wheel, as well as the elastic mechanical properties of the wheel surface and the supporting surface.

The derived analytical dependencies serve as a basis for further analysis of the nature of the contact interaction. Specifically, for deriving analytical relationships for the dimensions of the contact zones, the rolling resistance coefficient for deformable bodies, changes in the stress-strain state of the wheel and the supporting surface, as well as the limit load conditions that would lead to the failure of the supporting surface or the wheel [12, 13].

Relative to empirical methodologies, analytical frameworks generally offer superior scope and accuracy in quantifying the parameters governing contact interactions. Furthermore, these theoretical approaches yield a more comprehensive understanding of the mechanics of contact between deformable bodies, thereby enabling the optimization of interaction parameters and operational modes.

3. Results and Discussion

In the general case of the interaction of a deformable wheel with soil, the diagram of the forces acting on the soil can be represented by the diagram (Fig. 1).

To analyze the interaction of a deformable wheel with a deformable surface, a contact problem needed to be solved. This will allow to determine the contact surface deformations, the contact zone dimensions, and the force characteristics in the contact zone.

In the general case of solving a contact problem, when distributed forces act on the surface, the following biharmonic potential functions can be used [14]:

$$F1=\iint px\left[\xi,\eta\right]\Omega\mathrm{d}\xi\mathrm{d}\eta;\ G1=\iint py\left[\xi,\eta\right]\Omega\mathrm{d}\xi\mathrm{d}\eta;$$
$$H1=\iint pz\left[\xi,\eta\right]\Omega\mathrm{d}\xi\mathrm{d}\eta;\ \Omega=z\log\left[\rho+z\right]-\rho,$$
$$\rho\to\sqrt{\left(\left(x-\xi\right)^2+\left(y-\eta\right)^2+z^2\right)}, \quad (1)$$

where $px\left[\xi,\eta\right]$, $py\left[\xi,\eta\right]$, $pz\left[\xi,\eta\right]$ components of forces are distributed over the contact surface in the coordinate system x, y, z.

The following functions must also be considered:

$$F=\frac{dF1}{dz}=\iint px\left[\xi,\eta\right]\log\left[\rho+z\right]\mathrm{d}\xi\mathrm{d}\eta;$$
$$G=\frac{dG1}{dz}=\iint py\left[\xi,\eta\right]\log\left[\rho+z\right]\mathrm{d}\xi\mathrm{d}\eta;$$
$$H=\frac{dH1}{dz}=\iint pz\left[\xi,\eta\right]\log\left[\rho+z\right]\mathrm{d}\xi\mathrm{d}\eta. \quad (2)$$

In addition, it is possible to add the sums of the functions described above:

$$\psi1=\frac{dF1}{dx}+\frac{dG1}{dy}+\frac{dH1}{dz}=\frac{d\iint px\left[\xi,\eta\right]\Omega\mathrm{d}\xi\mathrm{d}\eta}{dx}+$$
$$+\frac{d\iint py\left[\xi,\eta\right]\Omega\mathrm{d}\xi\mathrm{d}\eta}{dy}+\frac{d\iint pz\left[\xi,\eta\right]\Omega\mathrm{d}\xi\mathrm{d}\eta}{dz};$$
$$\psi=\frac{d\psi1}{dz}=\frac{dF}{dx}+\frac{dG}{dy}+\frac{dH}{dz};$$
$$\frac{d\psi1}{dz}=\frac{d\iint px\left[\xi,\eta\right]\log\left[\rho+z\right]\mathrm{d}\xi\mathrm{d}\eta}{dx}+$$
$$+\frac{d\iint py\left[\xi,\eta\right]\log\left[\rho+z\right]\mathrm{d}\xi\mathrm{d}\eta}{dy}+\frac{d\iint pz\left[\xi,\eta\right]\log\left[\rho+z\right]\mathrm{d}\xi\mathrm{d}\eta}{dz}. \quad (3)$$

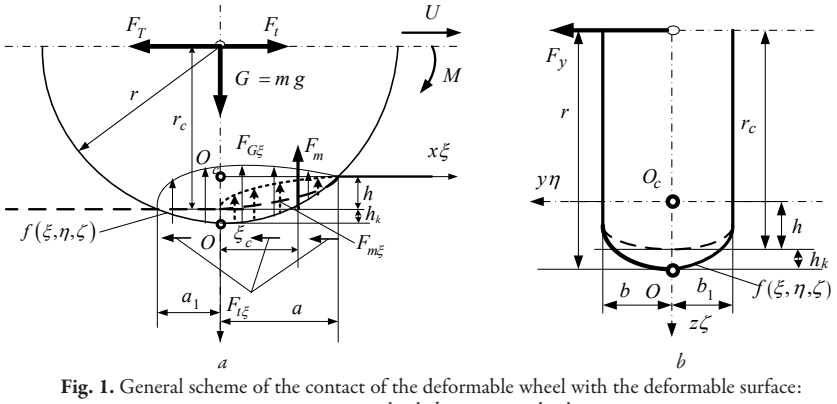

Fig. 1. General scheme of the contact of the deformable wheel with the deformable surface: *a* – active wheel; *b* – passive wheel

ISSN-L 2664-9969; E-ISSN 2706-5448

The surface displacement in the contact zone is expressed through the introduced functions as follows [15]:

$$u=\frac{1}{4\pi G}\left(2\frac{dF}{dz}-\frac{dH}{dx}+2\nu\frac{d\psi 1}{dx}-z\frac{d\psi}{dx}\right);$$
$$v=\frac{1}{4\pi G}\left(2\frac{dG}{dz}-\frac{dH}{dy}+2\nu\frac{d\psi 1}{dy}-z\frac{d\psi}{dy}\right);$$
$$w=\frac{1}{4\pi G}\left(2\frac{dH}{dz}+(1-2\nu)\psi-z\frac{d\psi}{dz}\right), \quad (4)$$

where u, v, w – displacement components in the x, y, z directions, respectively; G – modulus of elasticity of shear deformations of the surface body (material); ν – coefficient of lateral expansion (for elastic deformations – Poisson's ratio).

In expanded form, the displacement components will look like this:

$$w=\frac{1}{4\pi G}\left(\begin{array}{l}2\dfrac{d\iint pz[\xi,\eta]\log[\rho+z]\mathrm{d}\xi\mathrm{d}\eta}{dz}+\\+(1-2\nu)\left(\begin{array}{l}\dfrac{d\iint px[\xi,\eta]\log[\rho+z]\mathrm{d}\xi\mathrm{d}\eta}{dx}+\\+\dfrac{d\iint py[\xi,\eta]\log[\rho+z]\mathrm{d}\xi\mathrm{d}\eta}{dy}+\\+\dfrac{d\iint pz[\xi,\eta]\log[\rho+z]\mathrm{d}\xi\mathrm{d}\eta}{dz}\end{array}\right)-\\-z\left(\begin{array}{l}\dfrac{dd\iint px[\xi,\eta]\log[\rho+z]\mathrm{d}\xi\mathrm{d}\eta}{dzdx}+\\+\dfrac{dd\iint py[\xi,\eta]\log[\rho+z]\mathrm{d}\xi\mathrm{d}\eta}{dzdy}+\\+\dfrac{dd\iint pz[\xi,\eta]\log[\rho+z]\mathrm{d}\xi\mathrm{d}\eta}{dzdz}\end{array}\right)\end{array}\right); \quad (5)$$

$$v=\frac{1}{4\pi G}\left(\begin{array}{l}2\dfrac{d\iint py[\xi,\eta]\log[\rho+z]\mathrm{d}\xi\mathrm{d}\eta}{dz}-\\-\dfrac{d\iint pz[\xi,\eta]\log[\rho+z]\mathrm{d}\xi\mathrm{d}\eta}{dy}+\\+2\nu\left(\begin{array}{l}\dfrac{dd\iint px[\xi,\eta]\Omega\mathrm{d}\xi\mathrm{d}\eta}{dydx}+\\+\dfrac{dd\iint py[\xi,\eta]\Omega\mathrm{d}\xi\mathrm{d}\eta}{dydy}+\\+\dfrac{dd\iint pz[\xi,\eta]\Omega\mathrm{d}\xi\mathrm{d}\eta}{dydz}\end{array}\right)-\\-z\left(\begin{array}{l}\dfrac{dd\iint px[\xi,\eta]\log[\rho+z]\mathrm{d}\xi\mathrm{d}\eta}{dydx}+\\+\dfrac{dd\iint py[\xi,\eta]\log[\rho+z]\mathrm{d}\xi\mathrm{d}\eta}{dydy}+\\+\dfrac{dd\iint pz[\xi,\eta]\log[\rho+z]\mathrm{d}\xi\mathrm{d}\eta}{dydz}\end{array}\right)\end{array}\right); \quad (6)$$

$$u=\frac{1}{4\pi G}\left(\begin{array}{l}2\dfrac{d\iint px[\xi,\eta]\log[\rho+z]\mathrm{d}\xi\mathrm{d}\eta}{dz}-\\-\dfrac{d\iint pz[\xi,\eta]\log[\rho+z]\mathrm{d}\xi\mathrm{d}\eta}{dx}+\\+2\nu\left(\begin{array}{l}\dfrac{dd\iint px[\xi,\eta]\Omega\mathrm{d}\xi\mathrm{d}\eta}{dxdx}+\\+\dfrac{dd\iint py[\xi,\eta]\Omega\mathrm{d}\xi\mathrm{d}\eta}{dxdy}+\\+\dfrac{dd\iint pz[\xi,\eta]\Omega\mathrm{d}\xi\mathrm{d}\eta}{dxdz}\end{array}\right)-\\-z\left(\begin{array}{l}\dfrac{d\iint px[\xi,\eta]\log[\rho+z]\mathrm{d}\xi\mathrm{d}\eta}{dxdx}+\\+\dfrac{d\iint py[\xi,\eta]\log[\rho+z]\mathrm{d}\xi\mathrm{d}\eta}{dxdy}+\\+\dfrac{d\iint pz[\xi,\eta]\log[\rho+z]\mathrm{d}\xi\mathrm{d}\eta}{dxdz}\end{array}\right)\end{array}\right). \quad (7)$$

The differentials included in the equations (5)–(7) will look like:

$$dz=\partial_z\left(\frac{\log[\rho+z]}{\rho}\to\sqrt{\left((x-\xi)^2+(y-\eta)^2+z^2\right)}\right);\ dz=\frac{1}{\rho};$$
$$dx=\partial_x\left(\frac{\log[\rho+z]}{\rho}\to\sqrt{\left((x-\xi)^2+(y-\eta)^2+z^2\right)}\right);\ dx=\frac{x-\xi}{(z+\rho)\rho};$$
$$dy=\partial_y\left(\frac{\log[\rho+z]}{\rho}\to\sqrt{\left((x-\xi)^2+(y-\eta)^2+z^2\right)}\right);\ dy=\frac{y-\eta}{(z+\rho)\rho};$$
$$dxx=-\frac{\begin{array}{l}z(x-\xi)^2\rho-2z(x-\xi)^2\rho^{3/2}+z\rho^3+\rho^4+\\+\left(\begin{array}{l}z^2(x-\xi)^2+2z(x-\xi)^2\rho-\\-\left(z^2+(x-\xi)^2\right)\rho^2+\rho^4\end{array}\right)\log[z+\rho]\end{array}}{\rho^3(z+\rho)^2};\ \ldots\ dzz=\ldots. \quad (8)$$

Following the last expression, the second differentials have the fourth order of smallness and can be neglected. Then, the equations for the displacements will have the following form:

$$w=\frac{1}{4\pi G}\left(\begin{array}{l}2\iint pz[\xi,\eta]\dfrac{1}{\rho}\mathrm{d}\xi\mathrm{d}\eta+(1-2\nu)\times\\\times\left(\begin{array}{l}\iint px[\xi,\eta]\dfrac{x-\xi}{(z+\rho)\rho}\mathrm{d}\xi\mathrm{d}\eta+\\+\iint py[\xi,\eta]\dfrac{y-\eta}{(z+\rho)\rho}\mathrm{d}\xi\mathrm{d}\eta+\\+\iint pz[\xi,\eta]\dfrac{1}{\rho}\mathrm{d}\xi\mathrm{d}\eta\end{array}\right)\end{array}\right);$$
$$v=\frac{1}{4\pi G}\left(2\iint py[\xi,\eta]\frac{1}{\rho}\mathrm{d}\xi\mathrm{d}\eta-\iint pz[\xi,\eta]\frac{y-\eta}{(z+\rho)\rho}\mathrm{d}\xi\mathrm{d}\eta\right);$$
$$u\to\frac{1}{4\pi G}\left(2\iint px[\xi,\eta]\frac{1}{\rho}\mathrm{d}\xi\mathrm{d}\eta-\iint pz[\xi,\eta]\frac{x-\xi}{(z+\rho)\rho}\mathrm{d}\xi\mathrm{d}\eta\right). \quad (9)$$

In the absence of lateral forces $py[\xi,\eta]=0$, the equations will take a simpler form:

$$w=-\frac{1}{4G\pi}\iint\frac{(-1+2\nu)(x-\xi)px+(-3+2\nu)(z+\rho)pz}{\rho(z+\rho)}\mathrm{d}\xi\mathrm{d}\eta;$$

$$u=\frac{1}{4\pi G}\left(2\iint px\frac{1}{\rho}\mathrm{d}\xi\mathrm{d}\eta-\iint pz\frac{x-\xi}{(z+\rho)\rho}\mathrm{d}\xi\mathrm{d}\eta\right),$$

$$\rho=\sqrt{\left((x-\xi)^2+(y-\eta)^2+z^2\right)}. \quad (10)$$

Thus, to solve the problem of finding the absolute deformations of the wheel surfaces and the supporting surface, it is necessary to determine the components of the forces distributed over the surface.

The surface equation in the contact zone can be represented by functions in implicit form for the wheel and the surface:

$$fn=\zeta n-h+\frac{l^2\xi^2}{r}+\frac{k^2\eta^2}{r};$$

$$fk=\zeta k-hk+\frac{l^2\xi^2}{r}+\frac{k^2\eta^2}{r}, \quad (11)$$

where ξ,η,ζ *idem* x, y, z – coordinates of the wheel surface and the support surface in the contact zone; r – wheel radius; h – residual deformation of the support surface; hk – residual deformation of the wheel surface; l, k – deviation coefficients of the contact surface from spherical form (sphericity).

In explicit form, it will look like this (Fig. 2):

$$\zeta n=h-\frac{l^2\xi^2}{r}-\frac{k^2\eta^2}{r};$$

$$\zeta k=hk-\frac{l^2\xi^2}{r}-\frac{k^2\eta^2}{r}. \quad (12)$$

Concentrated forces act on the support surface from the *wheel side*. Moreover, they are balanced by the reactions of the support surface.

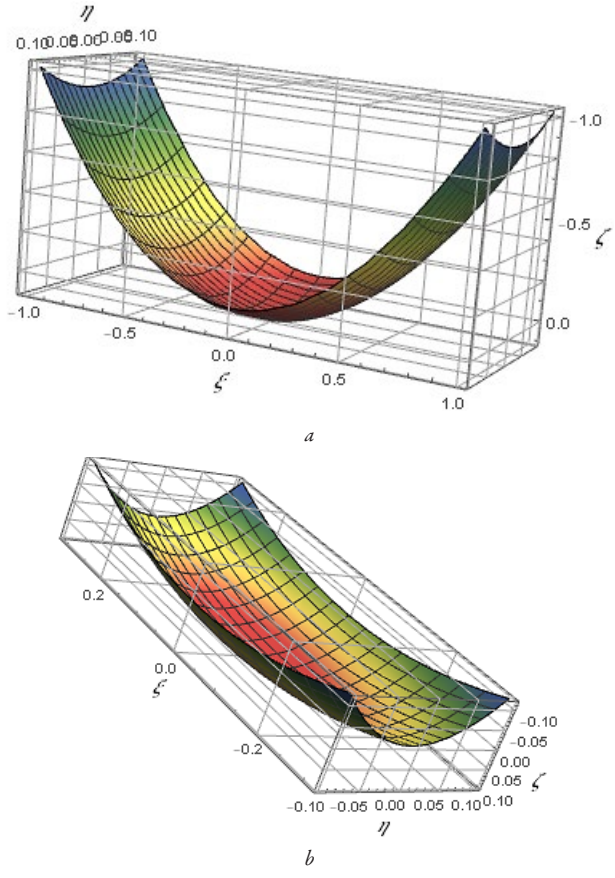

Fig. 2. View of the contact surface: *a* – contact surface with a larger length; *b* – contact surface with a smaller length

In this case, a flat formulation of the problem can be considered. In this case, the projections of forces will act on the vertical axis Oz and the horizontal axis Ox. The following forces from the side of the wheel act in the projection on the horizontal axis Ox:

– Horizontal driving component along the axis Ox. It acts on the entire length of the contact zone $\{a1;a\}$

$$F_{mtk}=M_c/(r-h_k), \quad (13)$$

where M_c – the torque on the drive wheel axis; r – wheel radius; h_k – residual deformation of the wheel.

– Traction resistance which is applied to the wheel axis and transmitted to the contact zone. It acts on the section $\{a1;a\}$: F_T.

– Horizontal component of rolling resistance. This force acts on the section $\{a1;a\}$ and will be defined in a separate section.

– Horizontal component of friction forces acting on the section $\{a1;a\}$

$$F_{ftk}=G\cdot f_t=m\cdot g\cdot f_t, \quad (14)$$

where f_t – friction coefficient; m – mass reduced to the wheel. The signs of friction forces have the following operator: "+" – active wheel, "–" – passive wheel.

– Vertical gravity component (acting on the section $\{a1;a\}$)

$$G_k=-m\cdot g; \quad (15)$$

for a wheel $\{a;a1\}->$ "–"; for a support $\{a;a1\}->$ "+".

– Vertical torque driving force component (acting on the section $\{0;a\}$)

$$F_{zk}=M_c/((a+0)/2); \quad (16)$$

for a wheel on the section $\{0;a\}$ – "–", $\{a1;0\}$ – 0; for a support $\{0;a\}$ – "+", $\{a1;0\}$ – 0.

– Vertical traction component (acting on the section $\{a1;0\}$)

$$F_{ztk}=F_T((a+a1)/2)/(r-h_k); \quad (17)$$

for a wheel on the section $\{0;a\}$ – "–", $\{0;a1\}$ – "+"; for a support $\{0;a\}$ – "–", $\{0;a1\}$ – "+".

– The vertical pushing force component for a passive wheel (acting on the section $\{0;a\}$)

$$F_{ztk}=F_t((a+0)/2)/(r-h_k); \quad (18)$$

for a wheel $\{0;a\}$ – "+", $\{0;a1\}$ – 0; for a support $\{0;a\}$ – "+", $\{0;a1\}$ – 0.

– Vertical rolling resistance (acting on the section $\{a1;a\}$)

$$M_{fmk}=F_{mk}\cdot\xi_c, \quad (19)$$

where ξ_c – geometric center (in the direction of the Ox axis ($o\xi$)) of applied sum of vertical loads distributed over the contact patch.

The concentrated forces for the *support surface* are similar to those given above, but differ in the operators mentioned above.

Considering the characteristics of the surface integral of the second kind, it is possible to formulate an equation to determine the distribution of forces over the contact surface:

$$\partial_\xi\partial_\eta\frac{\sum Fn}{s}=\partial_\xi\partial_\eta\iint_s F\xi\eta n\sqrt{1+(\partial_\xi fn)^2+(\partial_\eta fn)^2}\,\mathrm{d}\eta\mathrm{d}\xi;$$

$$\partial_\xi\partial_\eta\frac{\sum Fk}{s}\to\partial_\xi\partial_\eta\iint_s F\xi\eta k\sqrt{1+(\partial_\xi fk)^2+(\partial_\eta fk)^2}\,\mathrm{d}\eta\mathrm{d}\xi, \quad (20)$$

where s – contact zone area.

ISSN-L 2664-9969; E-ISSN 2706-5448

From the last equations, after differentiation, the equations for determining the forces distributed over the contact surface can be obtained:

$$\frac{\sum Fn}{s}=F\xi\eta n\sqrt{1+\left(\partial_{\xi}\zeta n\right)^2+\left(\partial_{\eta}\zeta n\right)^2};$$
$$\frac{\sum Fk}{s}=F\xi\eta k\sqrt{1+\left(\partial_{\xi}\zeta k\right)^2+\left(\partial_{\eta}\zeta k\right)^2}. \quad (21)$$

$$dfk=\frac{d^2}{d\xi d\eta}\sqrt{1+\left(\partial_{\xi}\zeta k\right)^2+\left(\partial_{\eta}\zeta k\right)^2}=\sqrt{\frac{r^2+4k^4\eta^2+4l^4\xi^2}{r^2}};$$
$$dfn=\frac{d^2}{d\xi d\eta}\sqrt{1+\left(\partial_{\xi}\zeta n\right)^2+\left(\partial_{\eta}\zeta n\right)^2}=\sqrt{\frac{r^2+4k^4\eta^2+4l^4\xi^2}{r^2}}. \quad (22)$$

Considering the transcendence in the last equations, which will cause difficulties in their integration, they can be expanded in a Maclaurin series

$$ndf=$$
$$=Normal\left[Series\left[\left(\frac{1}{\sqrt{\frac{r^2+4k^4\eta^2+4l^4\xi^2}{r^2}}}\right),\{\xi,0,2\},\{\eta,0,2\}\right]\right]=$$
$$=1-\frac{2\xi^2}{r^2}-\frac{2k^4\eta^2\left(r^2-6\xi^2\right)}{r^4}. \quad (23)$$

The coincidence of the real function and its expansion in a series within the length of the possible contact zone is evidenced by the graphs in Fig. 3.

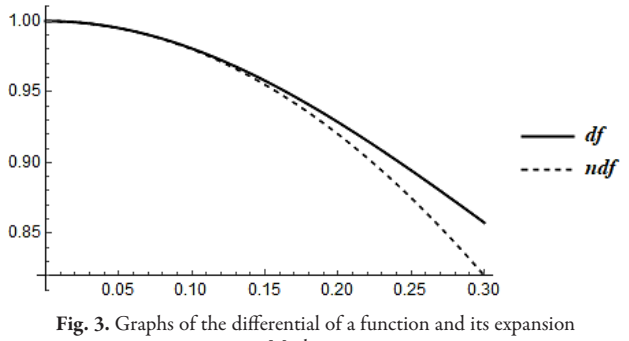

Fig. 3. Graphs of the differential of a function and its expansion in a Maclaurin series

The equation for the horizontal component of the distributed force on the wheel will look like

$$\frac{F_{tk}+F_{ftk}+F_t-F_T}{\left(a-a1\right)\left(b-b1\right)}=F_{xk}\,ndfk, \quad (24)$$

where F_{xk} – the horizontal projection of forces distributed over the wheel contact zone. From this equation, it is possible to obtain

$$F_{xk}=\frac{F_t-F_T+f_{tgm}+\frac{M_c}{h_k-r}}{\left(a-a1\right)\left(b-b1\right)}\left(1-\frac{2\xi^2}{r^2}-\frac{2k^4\eta^2\left(r^2-6\xi^2\right)}{r^4}\right). \quad (25)$$

For the vertical component, as described above, the force components are distributed over the sections $\{a1;0\},\{0;a\}$, which means the following equation can be written

$$\frac{-G}{\left(a-a1\right)\left(b-b1\right)}+\frac{-F_{zk}}{\left(0-a1\right)\left(b-b1\right)}+$$
$$+\frac{-F_{Tk}}{\left(0-a1\right)\left(b-b1\right)}+\frac{-F_{tz}}{\left(a-0\right)\left(b-b1\right)}=F_{zk}\,ndfk. \quad (26)$$

Hence, the distributed vertical component of the forces acting on the wheel can be expressed as follows

$$F_{zk}=\frac{-F_{Tk}-gm-\frac{M_c}{a}+\frac{aF_t}{h_k-r}}{\left(a-a1\right)\left(b-b1\right)}\left(1-\frac{2\xi^2}{r^2}-\frac{2k^4\eta^2\left(r^2-6\xi^2\right)}{r^4}\right). \quad (27)$$

Similarly, for forces distributed over the surface, it can be expressed like this:

$$F_{xn}=F_{xnn}\left(1-\frac{2l^4\xi^2}{r^2}-\frac{2k^4\eta^2\left(r^2-2l^4\xi^2\right)}{r^4}\right),$$
$$F_{xnn}=\frac{F_t-F_T+\frac{M_c+f_t gm\left(h-r\right)}{h-r}}{\left(a-a1\right)\left(b-b1\right)}; \quad (28)$$

$$F_{zn}=F_{znn}\left(1-\frac{2l^4\xi^2}{r^2}-\frac{2k^4\eta^2\left(r^2-2l^4\xi^2\right)}{r^4}\right),$$
$$F_{znn}=\frac{a^2a1\left(F_t+F_T\right)+2a1M_c\left(-h+r\right)-a\left(\begin{array}{l}a1^2\left(F_t+F_T\right)+\\+a1\,gm\left(h-r\right)+\\+2M_c\left(-h+r\right)\end{array}\right)}{a\left(a-a1\right)a1\left(b-b1\right)\left(-h+r\right)}. \quad (29)$$

The graphical representation of these forces distributions is presented in Fig. 4.

Fig. 4 illustrates the distribution patterns of the horizontal F_{xk}, F_{xn} and vertical F_{zk}, F_{zn} components of the distributed forces on the wheel and the surface, respectively. These patterns indicate that the maximum force distribution occurs closer to the center of the axle, but with a slight shift in the direction of wheel rolling, which correlates well with the results of other researchers.

The obtained results enable the prediction of force distribution and stress-strain state changes within the contact zone between the wheel and the supporting surface. This provides a foundation for developing analytical dependencies to determine the contact zone boundaries and the rolling resistance coefficient for interactions between deformable bodies.

It is important to note that these solutions assume linear elasticity and may not be strictly exact, particularly as real-world materials like soil often exhibit elastic-viscoplastic behavior. Nevertheless, the elastic formulation remains valuable for understanding the fundamental nature of the wheel-surface interaction.

This analytical approach facilitates predicting the stress-strain state evolution in the contacting bodies. The analysis phase allows to determine how various forces acting on the wheel influence the interaction and how these forces are distributed within the contact zone. By employing biharmonic potential functions, expressions are derived to determine the absolute deformations at the contact zone between a deformable wheel and a deformable surface.

The applicability of this method is confined to conditions of material continuity and elastic deformation. It precludes the analysis of contact interactions once plastic deformation or material discontinuity occurs. However, the derived analytical dependencies can identify regions susceptible to plastic deformation and material discontinuity.

These analytical expressions are pivotal for deriving dependencies that define contact boundaries and rolling resistance. Furthermore, these relationships can be employed to optimize wheel geometry aimed at minimizing soil compaction and enhancing its traction characteristics.

Future research directions can be aimed at studying the sliding (or slipping) conditions at the wheel-support surface contact zone, intending to improve the operational efficiency of the wheeled system.

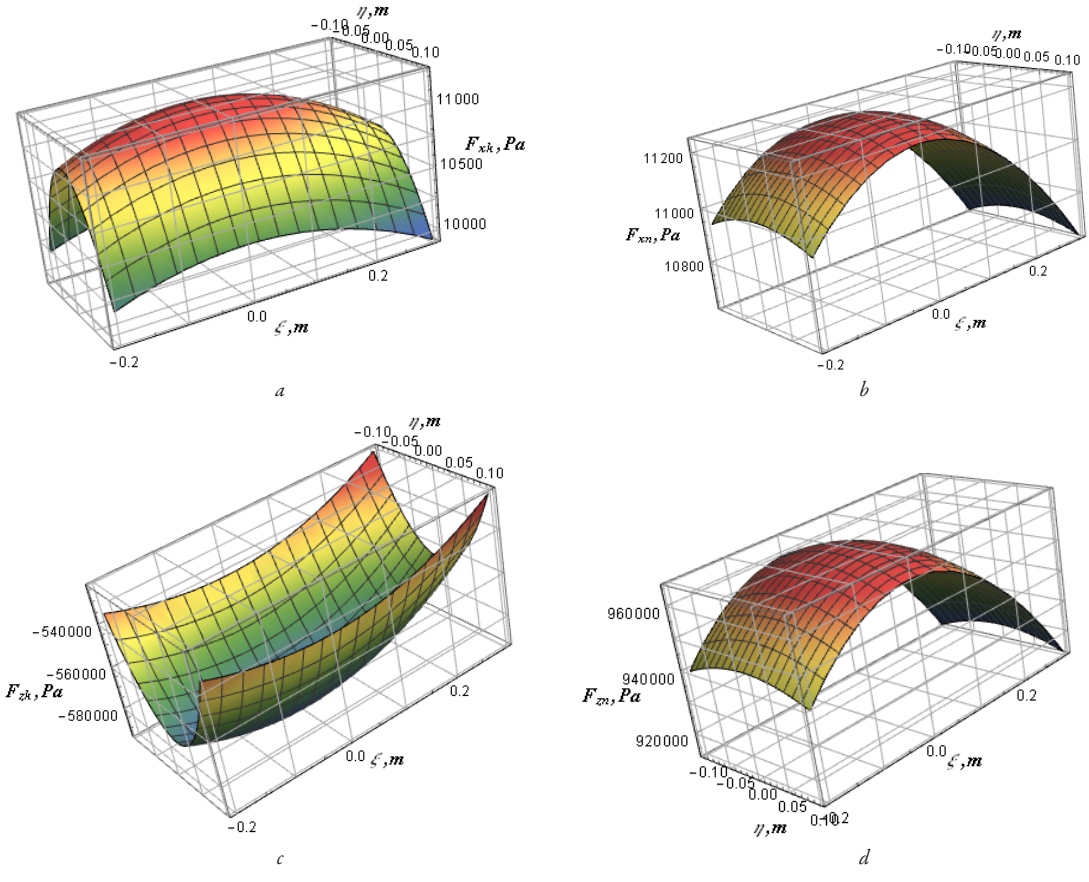

Fig. 4. Graphs depicting the distribution of forces over the contact interface between the wheel and the supporting surface: *a*, *b* – patterns of the horizontal components F_{xk}, F_{xn}; *c*, *d* – patterns of the vertical components F_{zk}, F_{zn}

4. Conclusions

Therefore, the equations of biharmonic potential functions for determining absolute deformations, in conjunction with the equations for forces distributed over the contact surface, yield a complex solution for the force distribution across the contact interface between the wheel (tire) and the supporting surface, incorporating the influence of concentrated forces acting on the wheel.

In this case, two possible variants of wheel rolling should be considered:

– on an active wheel, act the following forces and moments: M_c – torque on the drive wheel axis, the vertical component of gravity – $G_k = -m \cdot g$, traction resistance – F_T, i. e. the force expended on the traction of the towed vehicles, F_m – wheel rolling resistance, the horizontal component of friction forces – F_{fik};

– on a passive wheel act the following forces and moments: M_c – torque on the drive wheel axis, the vertical component of gravity – $G_k = -m \cdot g$, F_t – pushing force applied to the wheel axis, F_m – wheel rolling resistance, the horizontal component of friction forces – F_{fik}.

The obtained distributed force components are a basis for determining the absolute and relative deformations of the interacting wheel and supporting surface. They also allow to determine the stress distributions within both bodies and the characteristics of the contact patch dimensions, as well as the rolling resistance of the deformable wheel on the deformable surface.

The calculations mentioned above have yielded analytical dependencies for determining the absolute deformations of contacting bodies – specifically, the wheel (tire) and the deformable surface. These dependencies are functions of the bodies' mechanical properties (Young's modulus, Poisson's ratio) and the applied loads, applicable to both driving and driven wheels. This stems from the inherent features of the proposed contact problem-solving method, particularly the generality of its solution, which facilitates resolving contact tasks through analytical means. Based on the loads and material properties, these methods enable the selection of rational parameters for the deformable wheel, aiming to minimize excessive soil deformation and improve the wheel's tractive performance.

Employing the proposed analytical methods for contact interaction analysis eliminates the need for extensive computations typically required to achieve similar results via other means. Analytical solutions often surpass empirical methods in generality and accuracy for determining contact interaction parameters. They also enable a more complete characterization of contact mechanics in deformable bodies, facilitating the optimization of relevant parameters and interaction modes. Furthermore, unlike many computational techniques, these analytical solutions enable direct outcome prediction without resorting to time-consuming iterative procedures involving various load values and material properties of the contacting bodies.

In addition, the proposed model demonstrates this superiority by significantly increasing the accuracy of the analysis compared to empirical methods.

Conflicts of interest

The authors declare that they have no conflicts of interest in relation to the current research, including financial, personal, authorship, or any other, that could affect the research, as well as the results reported in this paper.

Financing

The research was conducted without financial support.

ISSN-L 2664-9969; E-ISSN 2706-5448

Data availability

All data are available, either in numerical or graphical form, in the main text of the manuscript.

Use of artificial intelligence

The authors confirm that they did not use artificial intelligence technologies when creating the current work.

References

1. Kushnarov, A. S., Kochev, V. I. (1989). *Mekhaniko-tekhnologicheskie osnovy obrabotki pochvy*. Kyiv: Urozhai, 144.
2. Kovbasa, V. P. (2006). *Mekhaniko-tekhnolohichne obgruntuvannia optymizatsii robochykh orhaniv z gruntom*. [Doctoral dissertation; Natsionalnyi universytet bioresursiv i pryrodokorystuvannia Ukrainy]. Available at: https://uacademic.info/ua/document/0506U000111#!
3. Koolen, A. J., Kuipers, H. (1983). *Agricultural Soil Mechanics*. Berlin: Springer-Verlag Berlin Heidelberg. https://doi.org/10.1007/978-3-642-69010-5
4. Swamy, V. S., Pandit, R., Yerro, A., Sandu, C., Rizzo, D. M., Sebeck, K., Gorsich, D. (2023). Review of modeling and validation techniques for tire-deformable soil interactions. *Journal of Terramechanics, 109,* 73–92. https://doi.org/10.1016/j.jterra.2023.05.007
5. Yang, W., Tiecheng, S., Yongjie, L., Chundi, S. (2016). Prediction for Tire – Pavement Contact Stress under Steady – State Conditions based on 3D Finite Element Method. *Journal of Engineering Science and Technology Review, 9 (4),* 17–25. https://doi.org/10.25103/jestr.094.04
6. Xiao, W., Zhang, Y. (2016). Design of manned lunar rover wheels and improvement in soil mechanics formulas for elastic wheels in consideration of deformation. *Journal of Terramechanics, 65,* 61–71. https://doi.org/10.1016/j.jterra.2016.03.004
7. Guthrie, A. G., Botha, T. R., Els, P. S. (2017). 3D contact patch measurement inside rolling tyres. *Journal of Terramechanics, 69,* 13–21. https://doi.org/10.1016/j.jterra.2016.09.004
8. Yamashita, H., Jayakumar, P., Alsaleh, M., Sugiyama, H. (2017). Physics-Based Deformable Tire–Soil Interaction Model for Off-Road Mobility Simulation and Experimental Validation. *Journal of Computational and Nonlinear Dynamics, 13 (2).* https://doi.org/10.1115/1.4037994
9. Bekker, M. G. (1969). *Introduction to Terrain-Vehicle Systems*. Ann Arbor: University of Michigan Press.
10. Pacejka, H. B. (2012). *Tire and Vehicle Dynamics*. Butterworth-Heinemann. https://doi.org/10.1016/C2010-0-68548-8
11. Kovbasa, V. P., Solomka, A. V., Spirin, A. V., Kucheruk, V. Yu., Karabekova, D. Zh., Khassenov, A. K. (2020). Theoretical determination of the distribution of forces and the size of the boundaries of the contact in the interaction of the deformable drive wheel with the soil. *Bulletin of the Karaganda University "Physics Series", 99 (3),* 62–72. https://doi.org/10.31489/2020ph3/62-72
12. Johnson, K. L. (1985). *Contact Mechanics*. London: Cambridge University Press. https://doi.org/10.1017/cbo9781139171731
13. Wong, J. Y. (2022). *Theory of Ground Vehicles*. Hoboken: John Wiley & Sons. https://doi.org/10.1002/9781119719984
14. Johnson, W., Mellor, P. B. (1973). *Engineering plasticity*. London, New York: Van Nostrand Reinhold Co.
15. Kovbasa, V., Priliepo, N. (2024). Interactions of a Deformable Wheel with a Deformable Support Surface. *International Journal of Innovative Technology and Exploring Engineering, 13 (9),* 1–4. https://doi.org/10.35940/ijitee.i9944.13090824

Volodymyr Kovbasa, *Doctor of Technical Sciences, Professor, Department of Mechanical and Electrical Engineering, Poltava State Agrarian University, Poltava, Ukraine, ORCID: https://orcid.org/0000-0003-4574-5826*

✉***Nataliia Priliepo,*** *Department of Mechanical and Electrical Engineering, Poltava State Agrarian University, Poltava, Ukraine, ORCID: https://orcid.org/0000-0002-4182-7405, e-mail: nataliia.pryliepo@pdau.edu.ua*

✉*Corresponding author*